Key Technologies for Energy Consumption Reduction of Aluminium Hydroxide Calciners

Wanqiu Cao[1], Zhiguo Li[2], Guohua Chen[3], Deming Yin[4] and Shengren Sun[5]
1. Director of Alumina Equipment Department
2. Vice General Manger
3. Manager of Alumina and New Materials Department
4. Vice Manager of R&D Center
5. Vice Director of Alumina Equipment Department
Shenyang Aluminium and Magnesium Engineering & Research Institute (SAMI), Shenyang, China
Corresponding author: zhg_li@chinalco.com.cn
https://doi.org/10.71659/icsoba2025-aa043

Abstract

This paper outlines the development and technological advancements in the calcination of aluminium hydroxide to produce Smelter Grade Alumina. It provides a detailed explanation of the physical and chemical reactions involved in the calcination process of aluminium hydroxide. In-depth research is conducted on improving separation efficiency, with a particular focus on analysing the inlet gas velocity of the cyclone separator and the insertion depth of the vortex finder. By optimizing the refractory lining design and materials, heat losses are reduced. Additionally, a novel low-temperature calcination technology is developed, which extends the residence time of the alumina in the high-temperature zone, thereby achieving reducing specific fuel energy and resulting carbon emissions.

Keywords: Calcination, Separation efficiency, Residence time, Energy consumption.

1. Introduction

Shenyang Aluminum & Magnesium Engineering & Research Institute (hereinafter referred to as SAMI) has accumulated extensive experience in the design, R&D, and production of alumina calciners through nearly 30 years of development and technological innovation. Currently, SAMI possesses the capability to design and develop alumina calciner equipment with capacities ranging between 500 and 6000 t/d (tonnes per day).

2. Development History of Alumina Hydrate Calciners

In the early stage of alumina production, rotary kilns were primarily used. Since rotary kilns have relatively high heat losses, high energy consumption and failure rates, they have gradually been replaced by gas suspension and circulating fluidized bed calciners [1].

The world's first gas suspension calciner for alumina was put into operation in 1986 by Denmark's FLSmidth at Hindalco Industries Limited, with a daily capacity of 1000 tonnes, replacing three rotary kilns [2]. China's first gas suspension calciner was introduced in 1987 by SAMI. After years of technological innovation, SAMI has improved their technological capabilities and developed their independent intellectual property. Currently, the largest single-capacity calciner in domestic production is 4000 tonnes per day, designed by SAMI and has been implemented in the Chongqing Jiulong Wanbo Project.

The first generation of alumina hydrate calciners adopted a vertical arrangement, as shown in Figure 1.

It mainly consists of four parts:

(1) Drying and preheating of raw materials (PO1, PO2)
(2) Calcination of raw materials (PO3, PO4)
(3) Primary air-cooling system (CO1-CO4)
(4) Secondary water-cooling system (KO1, KO2)

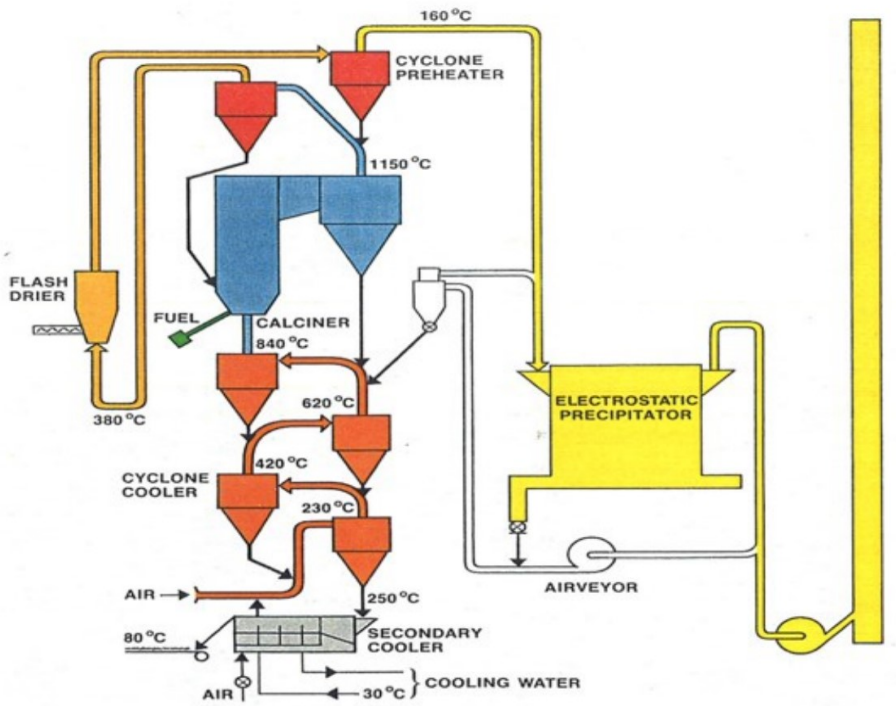

Figure 1. Vertical layout diagram of alumina calciner [2]**.**

Although most of rotary kilns have been replaced, some refineries have still implemented improvements on rotary kilns, as shown in Figure 2, to enhance heat recovery efficiency and reduce energy consumption.

With the advancement of design and technology, a calciner with a horizontal arrangement has been successfully developed, which significantly reduced the overall height of the calciner (as shown in Figure 3) and lowered the investment costs.

By 2013, with the increase in single production line capacity of alumina refineries, the demand for large-scale calciners became urgent. In 2015, SAMI successfully developed a 3500 tpd calciner with the largest single-unit capacity in China, which was successfully applied at Chalco Shanxi Huaxing Refinery and Xinfa Xiaoyi Refinery in 2016.

With the implementation of China's "Dual Carbon" strategy, energy-saving and carbon reduction objectives have become key directions for further research and development for alumina calciners.

Currently, the studies on reducing energy consumption at home and abroad mainly includes partial modifications and waste heat utilization. Among these, partial modifications mainly include the following aspects.

(1) Installing a cyclone separator before CO_2 backflow (alumina hydrate and alumina fine particles collected by dust collector) to separate the backflow cold air, which is then directed into the dust collection system, thereby reducing cold air ingress and minimizing heat loss.
(2) Reducing the moisture with the feedstock to decrease the heat consumption, thus lowering energy consumption.
(3) Extending the vortex finder of the cyclone PO1 to improve separation efficiency and reduce the backflow amount.

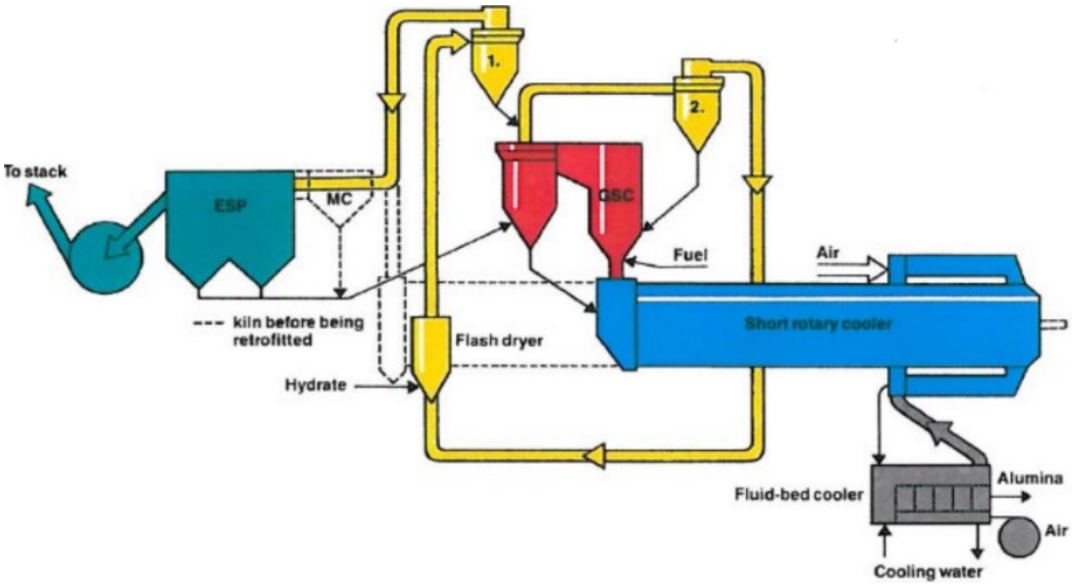

Figure 2. Schematic diagram of heat recovery modification in rotary kiln [3]

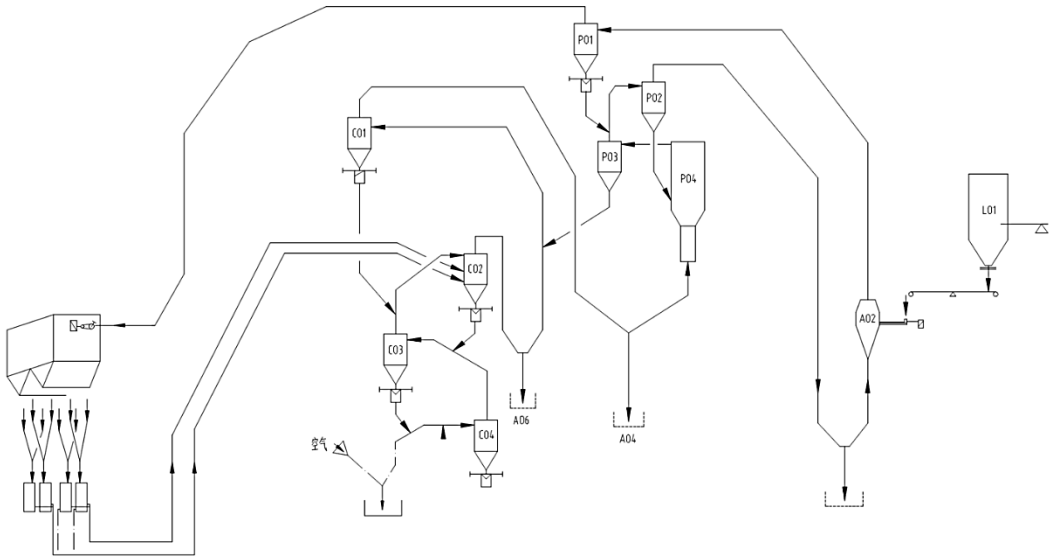

Figure 3. Horizontally arranged alumina hydrate calciner system.

Waste heat utilization primarily involves recovering heat from flue gas and the produced alumina. These studies fall under indirect heat recovery and do not truly reduce fuel consumption per tonne of alumina produced. Currently, waste heat recovery can be categorized into direct and indirect methods and is mainly used for heating hydrate filtration wash water or, in some cases also for room heating or bath water. The recovered heat is considerable and can reach 0.1 GJ/t Al_2O_3.

This paper will focus on a systematic study of the calciner system itself to explore methods of reducing the energy consumption of the calciner by investigating multiple factors such as gas-solid heat exchange efficiency, gas-solid heat transfer modes, gas-solid separation efficiency, and heat dissipation loss.

3. Process Principle of Alumina Calciners

The calcination process of moist aluminium tri-hydroxide (also called hydrate or gibbsite) involves drying the free surface moisture reacting the aluminium tri-hydroxide, and partially converting γ-alumina into α-alumina to meet the requirements of smelter grade alumina products. The reaction processes are as follows [4]:

(1) Removal of surface moisture and part of the hydroxides (pre-calcination):

$$2Al(OH)_3 + Heat \rightarrow Al_2O_3 \cdot 3H_2O\ (250–380\ ^\circ C) \quad (1)$$

(2) Decomposition of aluminium hydroxides (calcination):

$$Al_2O_3, xOH + Heat \rightarrow y\text{-}Al_2O_3 + (x\text{-}y)Al_2O_3\text{-}H_2O + yH_2O\ (380–1100\ ^\circ C) \quad (2)$$

(3) Crystal phase transformation (calcination):

$$\gamma\ Al_2O_3 \rightarrow \alpha\ Al_2O_3 + Heat\ (900–1100\ ^\circ C) \quad (3)$$

In the study on the phase transition from alumina hydrate to alumina, numerous outstanding results have been achieved, among which the work of Levin et al. [5] holds significant importance. Studies have found that the phase transition of alumina hydrate is influenced by multiple parameters (temperature, heating rate, residence time, particle diameter, impurities, etc.), with impurities (Na_2O, Fe_2O_3, SiO_2) primarily related to the process flow prior to calcination. In the initial stage, the reaction proceeds relatively rapidly, forming boehmite (aluminium oxy-hydroxides) or low order transition alumina forms. Subsequently, the hydroxide removal process becomes slower, and even with sufficient heat, extended heating time is required to generate the thermodynamically stable alpha alumina form.

Alumina hydrate calciners can account for more than 30 % of the total energy consumption in alumina refineries, so reducing energy consumption is an important measure to reduce overall carbon emissions. Currently, domestic gas suspension calciners typically operate at temperatures around 1050–1150 °C. This study employs multiple innovative technologies to lower the calcination temperature to below 950 °C, achieving significant energy savings and fuel consumption reduction. Additionally, nitrogen oxides (NOx) will be generated in the combustion process. The mechanism for nitrogen oxides generation is mainly thermal, that is, N_2 in the air is oxidized and generated in the high temperature environment [6]. Due to the different fuels, the content of nitrogen oxides generated varies greatly. Research indicates that when the temperature is lower than 1000 °C, the production of thermal nitrogen oxides will be greatly reduced. Therefore, reducing the calcination temperature is of great significance for decreasing NO_x emissions.

4. Study on Gas-Solid Heat Transfer Technology for Alumina Hydrate Calciners

The heat exchange efficiency of a calciner is affected by multiple factors, primarily depending on the uniformity of mixing between particles and gas phase, the heat exchange efficiency between

particles and gas phase, the heat capacity flow ratio of particles to gas, the contact between particles and gas, the number of stages in the heat exchanger, and the separation efficiency of the cyclone separators.

4.1 Uniformity of Mixing Between Particles and Gas Phase

In the riser of a cyclone separator, the effective dispersion or mixing of solid particles in the gas largely depends on the dispersion device (distributor), including its position in the riser, the momentum of solid particles upon entering the riser, and the flow field pattern. From the perspective of calciner system design, the location of the distributor and the momentum of solid particles must be optimized in conjunction with the layout of the calciner system, while also considering the economic efficiency of the calciner system to achieve uniform mixing of solid particles and the gas phase.

4.2 Heat Exchange Efficiency Between Particles and Gas Phase

The heat exchange efficiency between solid particles and the gas phase during contact time primarily depends on the heat transfer coefficient h, which is defined through the dimensionless Nusselt number as:

$$h = Nu \; {}^{k_g}\!/_{d_p} \tag{4}$$

where:
k_g thermal conductivity of the fluid (gas)
d_p particle diameter

The Nusselt number is related to the dynamic conditions of the fluid surrounding solid particles, i.e., whether each particle can be considered suspended in the gas phase with little or negligible interaction with other particles, or whether the particles are in a fluidized bed with significant interactions among them. It can be expressed according to the following Equation (5).

$$Nu = \; 2 + (0.6 \; or \; 1.8) \; Re_p^{0.5} \; Pr^{0.33} \tag{5}$$

where:
Re_p Reynolds number of the particle
Pr Prandtl number
0.6 correlation coefficient for isolated particles in a laminar flow
1.8 same coefficient for dense bed in a turbulent flow

The Reynolds number of the particle is related to the ratio of inertial forces to viscosity forces in the flow, it is expressed as:

$$Re_p = {}^{U_0 \; \rho_g \; d_p}\!/_{\mu} \tag{6}$$

where:
U_0 relative velocity of the fluid with respect to the particle
μ dynamic viscosity of the fluid
ρ fluid density

The relative velocity of the particles in a fluidised bed can be estimated with the following formula, resulting from typical sedimentation or free-fall models of a particle in a viscous fluid, taking into account the fluid resistance (drag).

$$U_0(t) = \frac{d_p^2\,(\rho_p - \rho_g)\,g}{18\,\mu}\left(1 - e^{-\frac{18\,\mu}{{d_p}^2\,\rho_p}t}\right) + U_{0i}\,e^{-\frac{18\,\mu}{{d_p}^2\,\rho_p}t} \tag{7}$$

where:
ρ_p particle density

The Prandtl number is related to the ratio between momentum diffusivity and thermal diffusivity, it is expressed as:

$$Pr = C_{pg}\,{}^{\mu}/_{k_g} \tag{8}$$

where:
C_{pg} specific heat capacity at constant pressure of the fluid

According to the above correlation in Equation (4), the heat transfer coefficient h can be calculated and Table 1 lists some values at different times.

Table 1 Theoretical heat transfer coefficients of particles during acceleration in gas.

Time (s)	U_{0i} (m/s)	Nu	h (W/m^{2}K)
0	20	5.4	6 200
0.01	4.7	3.6	4 200
0.076	0.07	2.2	2 544

To sum up, both the initial particle velocity and the particle diameter significantly impact the heat exchange efficiency. Therefore, when the particle diameter remains relatively constant, appropriately increasing the initial particle velocity while considering system resistance loss can effectively enhance heat exchange efficiency.

4.3 Heat Recovery and Heat Transfer Efficiency in Gas Suspension Calciners

The heat efficiency primarily depends on the heat capacity flow ratio between gas and solid phases, the contact mode, and the number of heat exchange stages.

4.3.1 Heat Capacity Flow Ratio Between Particles and Gas

The heat capacity flow ratio between particles and gas in a simple heat transfer process, such as in the cooling stage of an alumina gas suspension calciner system, is assumed under adiabatic conditions as follows:

$$SC_{\mathrm{ps}}\Delta T_{\mathrm{s}} = -GC_{\mathrm{pg}}\Delta T_{\mathrm{g}} \tag{9}$$

where:
S mass flow of the solid (alumina)
G mass flow of the gas (air)

C_{ps} specific heat of alumina at constant pressure
C_{pg} specific heat of air at constant pressure

The heat capacity flow ratio ⌀ is defined as:

$$\phi = -\frac{\Delta T_s}{\Delta T_g} = \frac{G}{S} \bullet \frac{C_{pg}}{C_{ps}} \tag{10}$$

The total air required for combustion for the four-stage cyclone cooler of the gas suspension calciner process is calculated as follows:

$$G = S\frac{K}{\Delta H_{com}}(1+E)\ \ \nu_{air} \Rightarrow \phi = \nu_{air}(1+E)\frac{K}{\Delta H_{com}}\frac{C_{pg}}{C_{ps}} \tag{11}$$

From the equations, it can be observed that in the cooler system of the gas suspension calciner, nearly all the combustion air is utilized to recover heat from the alumina in the heating system, resulting in a heat capacity flow ratio (⌀) of approximately 1. In the drying and pre-calcination stages of the gas suspension calciner, the heat capacity flow ratio (⌀) is approximately 0, the heat is primarily used for attached water evaporation and pre-calcination, and the solid-phase temperature is almost constant.

4.3.2 Contact Methods Between Particles and Gases

The relative flow and contact methods (cross-flow, counterflow, or fair flow) between particles and gases directly affect the heat efficiency of heat exchange processes. Generally, counterflow between gases and particles is a highly efficient contact mode and has been applied in rotary kilns. In gas suspension calciners, the counterflow contact between gas and solid phases can be achieved through multi-stage cyclone separators in series, while particle-gas contact is realized in fair flow, as shown in Figures 4(a) and 4(b). The cross-flow contact mode is shown in Figure 4(c). In alumina gas suspension calciners, the heat transfer mode as shown in Figure 4 (b) is adopted.

5. Study on Energy-saving and Carbon Reduction Technologies

The energy consumption reduction of alumina hydrate calciners is primarily related to the following aspects:

(1) Separation efficiency of gas-solid phase flow
(2) Heat dissipation loss
(3) Reduction of calcination temperature

5.1 Improving Gas-Solid Separation Efficiency

The separation efficiency of a cyclone separator is influenced by many factors, primarily including operational parameters and design parameters, such as the gas inlet velocity, the insertion depth of the vortex finder, the structure of the volute, and the cone angle. In this paper, two most influential factors, gas inlet velocity and the insertion depth of the vortex finder are simulated and analysed.

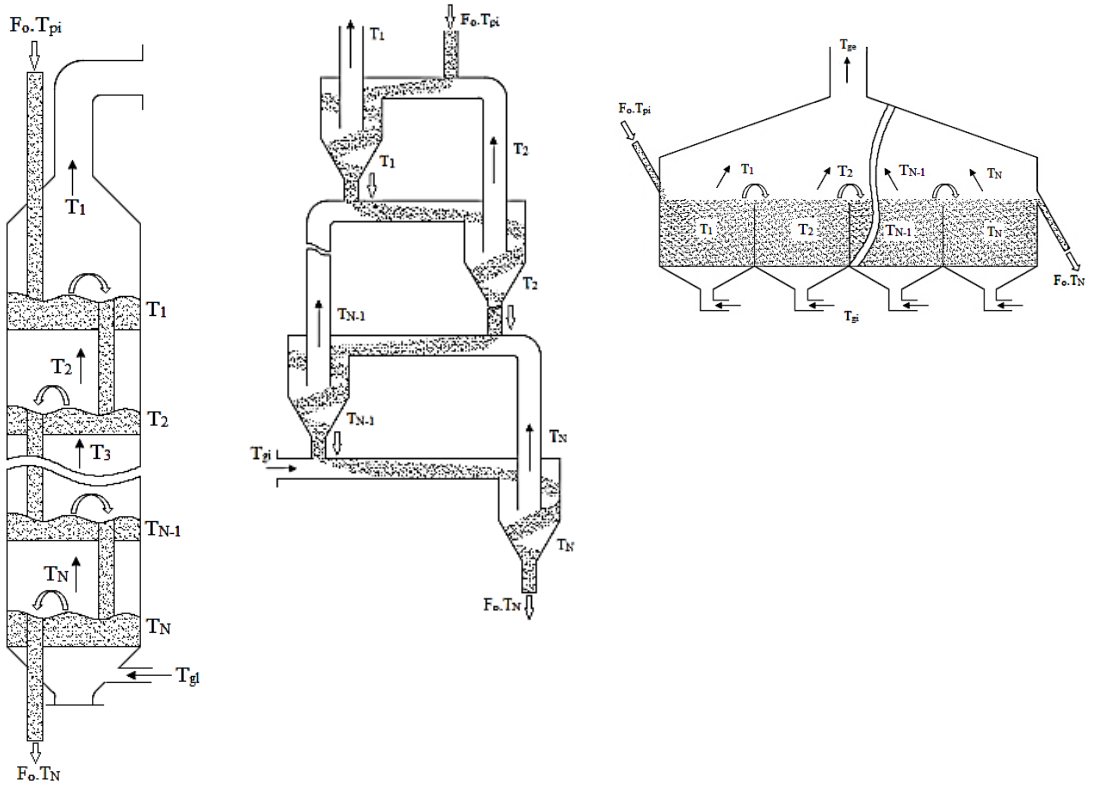

Figure 4. Gas-solid heat transfer modes [7].

5.1.1 Impact of Inlet Velocity on Separation Efficiency

On the basis of the same other conditions, a cyclone separator was simulated and analysed to study the separation efficiency when the inlet velocity was v = 12, 13, 14, and 16 m/s, the classification efficiency when the particle size was in the range of 1–120 μm, and the separation efficiency of alumina hydrate particles with Rosin-Rammler distribution. Through Fluent simulation analysis, Figure 5 illustrates the classification efficiency of alumina hydrate particles within the 1–120 μm range under different inlet velocities.

Table 2 lists the cut particle size d_{50} and critical particle size d_{100} under different inlet velocities, along with the separation efficiency according to the Rosin-Rammler distribution.

From Figure 5 and Table 2, it can be observed that as the inlet gas velocity increases, the separation efficiency of alumina hydrate particles also increase, while the cut particle size and critical particle size decrease. This indicates that increasing the inlet gas velocity significantly improves the separation efficiency of the cyclone separator. However, it is worth noting that further increasing the inlet gas velocity may lead to re-entrainment of particles already deposited on the cylinder wall due to turbulence and particle collisions, as well as severe backflow at the discharge port, resulting in a decline in separation efficiency. As shown in Table 2, when the velocity (v) reaches 16 m/s, the separation efficiency decreases instead of rising. Moreover, excessively high gas velocity can exacerbate particle breakage and wear of the cyclone internals. Studies have shown that the wear of cyclone separators is proportional to the fourth power of the gas velocity. Excessive inlet gas velocity not only increases resistance loss but also raises the excess air coefficient, lowering the primary calciner temperature and increasing heat loss through flue gas. Therefore, the inlet gas velocity must be determined appropriately based on the specific conditions of each cyclone separator. According to the cyclone separator simulated in this paper,

combined with the above analysis, it is considered that the separation efficiency is the optimal when the gas velocity is 13–14 m/s.

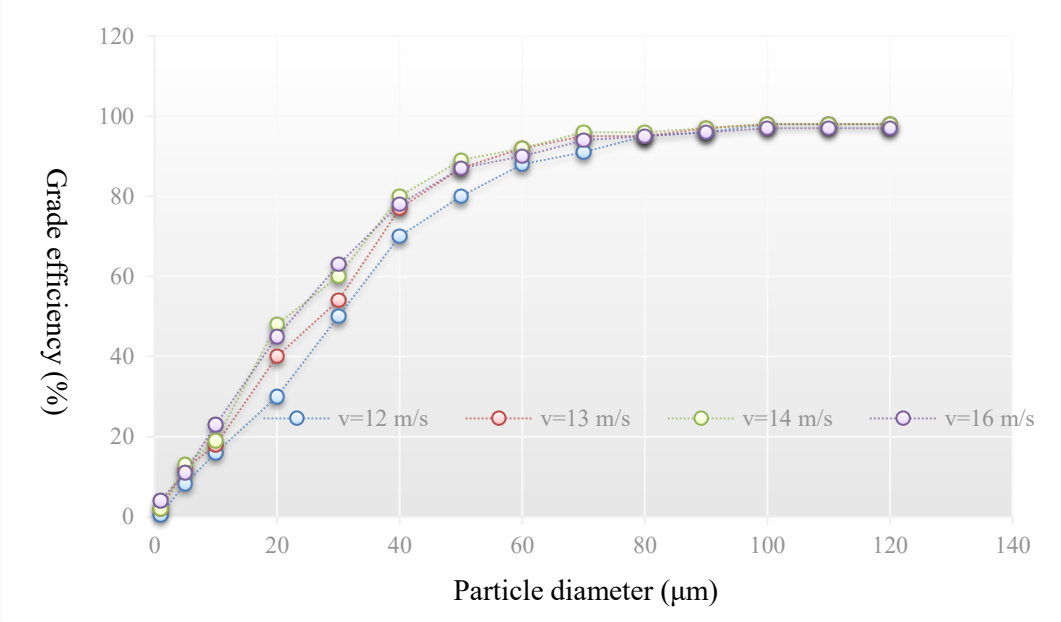

Figure 5. Impact of inlet velocity on classification efficiency.

Table 2. Separation efficiency under different inlet velocities.

Inlet velocity (m/s)	12	13	14	16
d_{50} (μm)	27.8	25.1	21.4	20.6
d_{100} (μm)	77.8	74.1	71.7	70.2
Classification efficiency $_{R\text{-}R}$ (%)	87.1	89.3	89.7	89.1

5.1.2 Impact of Vortex Finder Insertion Depth on Separation Efficiency

To study the effect of vortex finder insertion depth on the separation efficiency of a cyclone separator, the classification efficiency of alumina hydrate particles with particle sizes of 1–120 μm and the separation efficiency for alumina hydrate particles following a Rosin-Rammler distribution were studied at insertion depths of h = 1800 mm, 2100 mm, 2450 mm, and 2750 mm. Through Fluent simulations using a single-variable control analysis, Figure 6 illustrates the classification efficiency of alumina hydrate particles with the particle size of 1–120 μm at different vortex finder insertion depths. Table 3 lists the cut particle size d_{50} and critical particle size d_{100} for different insertion depths, along with the separation efficiency based on the Rosin-Rammler distribution

From the Figure 6 and Table 3, it can be observed that as the insertion depth of the gas riser increases, the separation efficiency of alumina hydrate particles improves, while the cut particle size and critical particle size decrease, indicating a significant enhancement in the cyclone separator's separating performance. This is because increasing the insertion depth of the vortex finder suppresses the short-circuit flow of dust-laden gas directly entering the vortex finder from the inlet, thereby improving the separation efficiency of the cyclone separator. However, the insertion depth of the vortex finder should not be excessive, as it would reduce the number of effective spiral rotations of the gas flow and increase the likelihood of secondary entrainment,

ultimately lowering separation efficiency. As shown in Table 3, when the insertion depth (h) of the vortex finder increases from 2 450 to 2 750, the separation efficiency of the cyclone separator decreases from 90.6 % to 89.3 % on the contrary. Therefore, it is essential to select an appropriate insertion depth of the vortex finder based on the specific conditions of each cyclone separator.

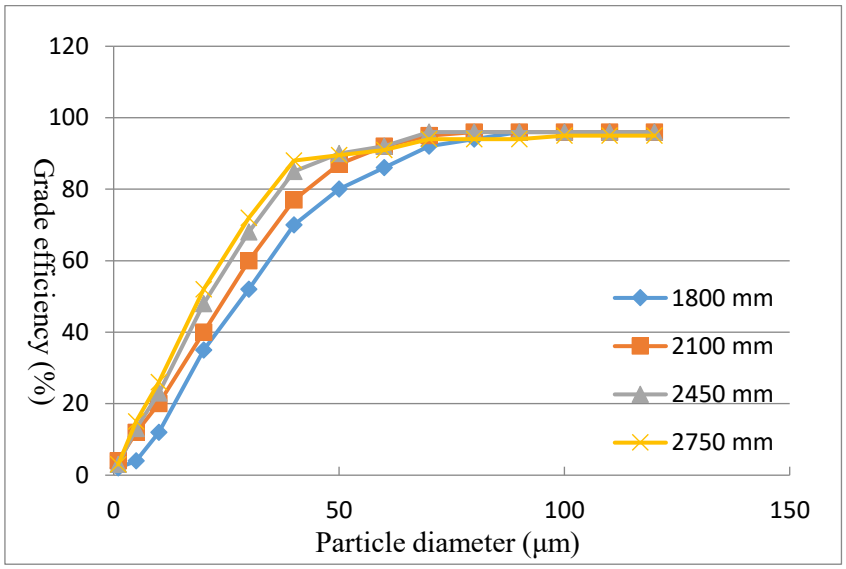

Figure 6. Impact of vortex finder insertion depth on classification efficiency.

Table 3. Separation efficiency under different vortex finder insertion depths.

Vortex finder insertion depth (mm)	1800	2100	2450	2750
d_{50} (μm)	25.7	24.3	20.2	18.8
d_{100} (μm)	75.4	73.7	65.4	53.6
Separation efficiency $_{R\text{-}R}$ (%)	87.2	88.4	90.6	89.3

5.2 Reducing Heat Dissipation Loss

Most researchers focusing on reducing energy consumption of alumina calciners typically prioritize improving heat exchange efficiency, while studies on refractory materials are often overlooked. The primary design objective of refractory materials is to reduce calciner wall temperature and extend the service life of the calciner body. Ideally, all heat in the calcination system should be utilized for removing free surface moisture and facilitating the endothermic calcination reactions. However, in practice, a significant amount of heat is lost in several ways: energy losses through cyclone separators, pipelines, and chutes under steady-state operating conditions, as well as heat storage losses during transient states.

Under steady-state conditions, the heat loss through the calciner wall depends on the thermal conductivity "K" of the refractory material, gas velocity, ambient temperature, surface temperature, emissivity, and operating temperature. Generally, materials with high porosity and low thermal conductivity reduce the service life of the refractory lining due to their lower strength and resistance to chemical erosion. Conversely, high-density refractory materials typically exhibit higher strength and longer lifespan, but their higher thermal conductivity leads to greater heat dissipation loss. Therefore, a multi-layer design using materials with lower thermal conductivity is necessary to minimize unnecessary heat loss. Refractory materials can also protect the steel shell from corrosion and erosion while providing thermal insulation. The multilayer lining should be selected rationally in the specific operating environment, and the performance of each layer

should be optimized to improve the thermal efficiency in the calciner and reduce the fuel consumption. In many existing alumina calciners, the designed refractory material typically consists of two or three layers, that is, two thermal insulation layers and one dense refractory material layer for hot surfaces. Operational experiences from multiple on-site calciners indicate that radiation heat loss through the cyclone furnace walls is significant, leading to higher energy consumption. This paper conducts a detailed study on the lining materials and their thicknesses, optimizing the refractory material thickness and selection through heat engineering calculations to enhance energy efficiency. The design and material selection of the refractory lining shall meet the following requirements:

(1) It shall withstand thermal shocks during emergency start-ups and shutdowns without significantly reducing the service life of the refractory material.
(2) It shall resist cold and hot abrasion from solids in gas suspension without significantly shortening the service life of the refractory material.
(3) It shall provide reliable long-term service life and low-cost maintainability.
(4) The anchor bolt structure and material selection shall be optimally designed to support the refractory material vertically and horizontally.

Meanwhile, accommodate the refractory material's movement due to thermal expansion. The lining before optimization is shown in Figure 7, the original lining structure form and its cooling curve are shown in Figure 8, and the optimized lining structure is shown in Figure 9.

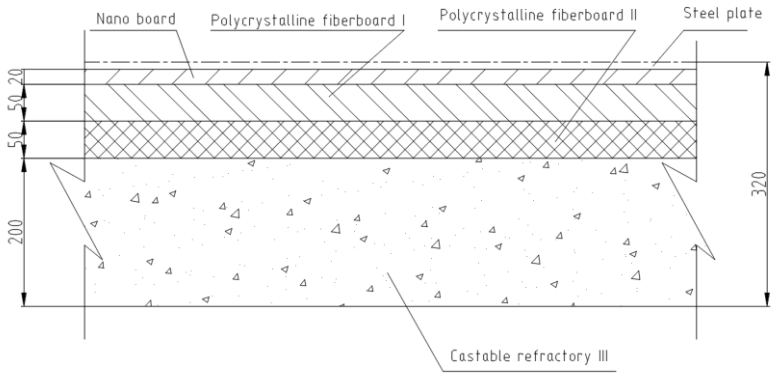

Figure 7. Original lining structure.

Table 4. Heat engineering calculation of original lining structure.

Ambient temperature ta	25 ℃	Furnace chamber temperature tk	1050 ℃
Gas velocity	0 m/s	Radiation coefficient	0.8
Insulation material	Insulation thickness (mm)	Hot side temperature °C	Cold surface temperature °C
Castable refractory III	200	1050	950.9
Polycrystalline board I	50	950.9	802.1
Polycrystalline board II	50	802.1	603.1
Nano board	20	603.1	78.7
Cold surface temperature tc			78.7
Heat dissipation loss Qc		708.4	W/m^2

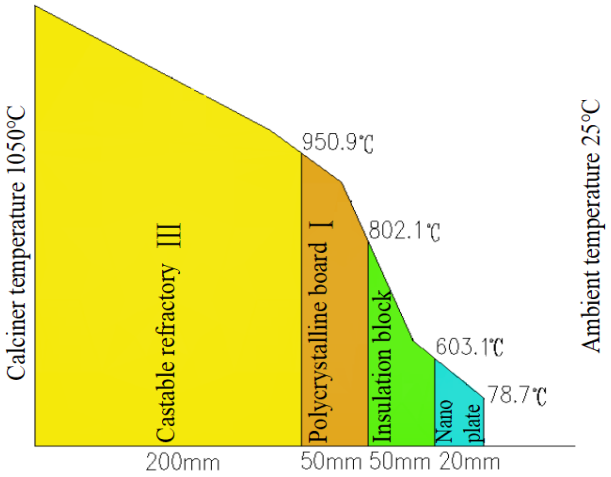

Figure 8. Cooling curve of original lining structure.

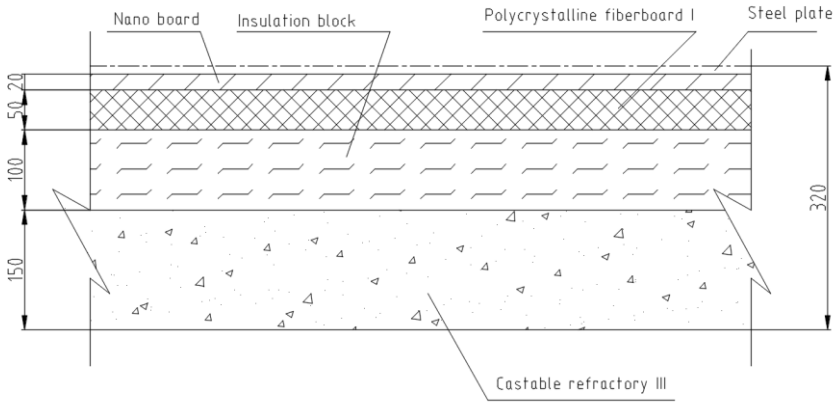

Figure 9. Optimized lining structure.

Table 5. Heat engineering calculation of optimized lining structure.

Ambient temperature t_a	25 ℃	Furnace chamber temperature tk	1050 ℃
Gas velocity	0 m/s	Radiation coefficient	0.8
Insulation material	Insulation thickness (mm)	Hot side temperature °C	Cold surface temperature °C
Castable refractory III	150	1050	994.5
Polycrystalline board I	50	994.5	893.0
Insulation block	100	893.0	485.5
Nano board	20	485.5	67.5
Cold surface temperature tc			67.5
Heat dissipation loss Qc		529.8	W/m^2

The cooling curve of the optimized lining structure is shown in Figure 10. Through calculation, the heat dissipation loss can be effectively reduced by approximately 15 % by adopting the multi-layer lining structure design and changing the lining material.

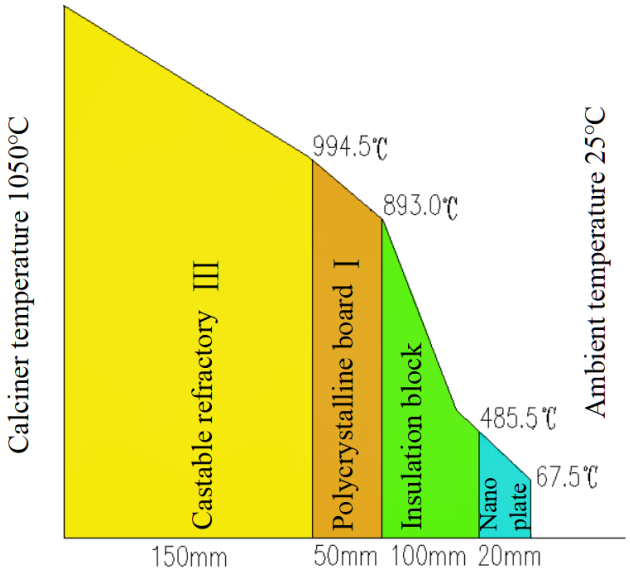

Figure 10. Cooling curve of optimized lining structure.

5.3 Low-temperature Calcination Technology

The domestic gas suspension calciners generally operate at a temperature range of around 1050–1150 °C, where the high calcination temperature leads to higher outlet temperature and flue gas temperature, resulting in greater heat loss. This paper proposes a low-temperature calcination technology that achieves reduced calcination temperature (even below 950 °C) by extending the residence time of materials in the high-temperature zone, thereby minimizing heat loss and lowering energy consumption.

The residence time can be extended to 5–15 minutes by using a fluidized residence tank, prolonging material residence time in the high-temperature zone. The residence time can be controlled by adjusting the fluidizing air flow rate. After further reaction in the residence tank, the material enters the cooling system, with the process flow shown in Figure 11.

The core equipment of low-temperature calcination technology is the residence tank (No. 16 in Figure 11), which addresses the key technical challenge of ensuring materials remain in a high-temperature fluidized state for a required duration without material sedimentation. Figure 12 presents the fluidization simulation results.

As shown figure 12, the particle phase is uniformly distributed with a good fluidization state, and no material sedimentation is observed.

The low-temperature calcination technology essentially does not change the existing process flow, so it has no fundamental impact on the stability and operability of the entire calcination system. This technology offers the following advantages:

1) The calcination temperature is reduced, the thermal energy consumption per unit product is reduced, and the operation cost is reduced.
2) The thickness of the lining can be reduced and the construction cost can be saved on the premise of maintaining the temperature of outer surface constant;
3) The outlet temperature is reduced, the cooling water volume of the fluidized bed is reduced, and the operation cost is reduced;
4) The calcination temperature is reduced, the amount of air required is reduced, the size

of equipment can be reduced, and the construction cost is reduced.

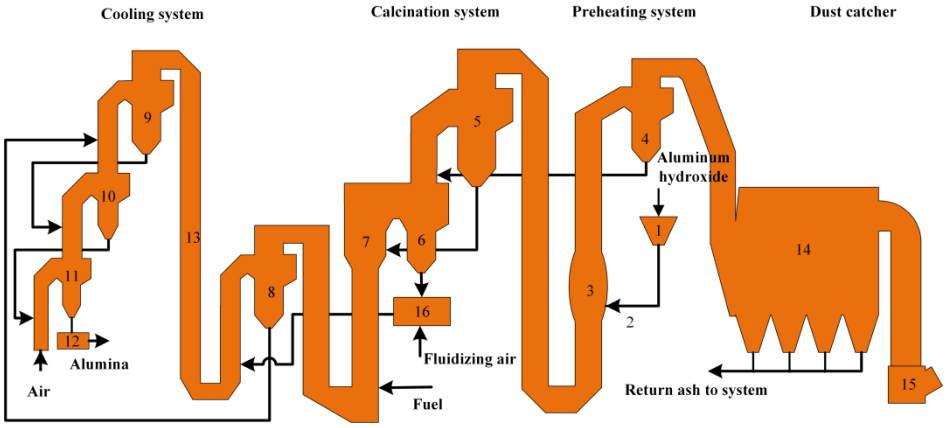

Figure 11. Process flow of low-temperature calcination (see Legend below). Legend: 1. Feed bin, 2. Feeding system, 3. Venturi dryer, 4–6. 1st–3rd stage cyclone preheaters, 7. Calciner, 8–11. 1st–4th stage cyclone coolers, 12. Fluidized bed cooler, 13. Connecting ducts, 14. Dust collector, 15. ID fan, 16. Residence tank.

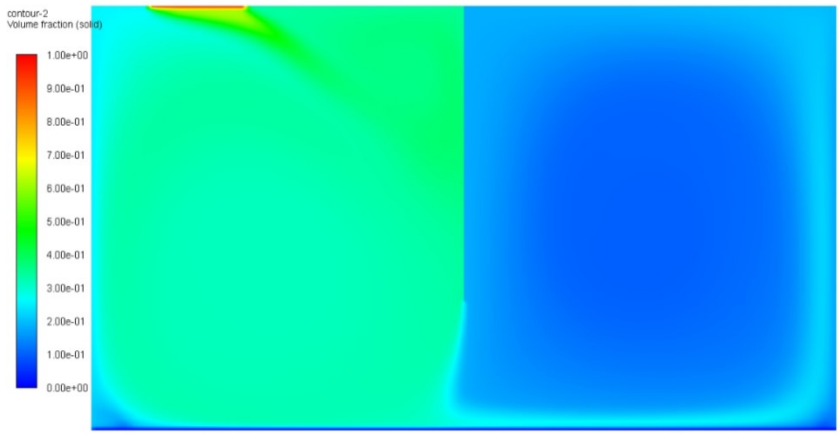

Figure 12. Fluidization numerical simulation of residence tank.

Currently, the specific fuel energy consumption of alumina calciners is approximately 3.0 GJ/t Al_2O_3. By applying this technology, the specific energy consumption can be reduced to 2.8 GJ/t Al_2O_3, achieving a reduction of about 0.2 GJ/t Al_2O_3. Calculated by a 1 Mt/y alumina production line, 5 460 tonnes of standard coal equivalent can be saved annually; calculated with a coal price of 800 RMB/t, the annual cost savings amount to 4.4 million RMB. When natural gas is used in the calcination process, the calciner's carbon emission per unit product is 168 kg. By adopting low-temperature calcination technology, a 1 Mt/y alumina refinery can reduce its annual CO_2 emissions by:

$$168 \times 1\,000\,000 \times 0.2/3.0/1000 = 11\,200 \text{ tonnes of } CO_2 \text{ per year}$$

Summary: the energy-saving and fuel consumption reduction theory proposed in this paper has been implemented in multiple alumina refineries for retrofitting, with theoretical results verified. Since the newly added or modified equipment is primarily static, long-term stable energy-saving and carbon reduction operation can be ensured. As mentioned earlier, the residence tank is a non-static equipment requiring material fluidization, which is achieved by a suspension fan, a mature and highly reliable equipment. As a result, a stable on-site operation can also be ensured.

6. Conclusion

This paper provides a brief overview of the history of the development of SAMI's alumina calciners, analyzes and summarizes the mechanisms of the calcination process, and focuses on the study of gas-solid heat transfer technology, heat transfer efficiency, the influence of refractory lining on heat dissipation losses, as well as energy-saving and carbon reduction technologies.

Through research and analysis, it has been found that adopting a multi-layer optimized refractory lining design can reduce heat loss by approximately 15 %. A technology for low-temperature calcination has been proposed, which can lower the calcination temperature by 100 °C, demonstrating significant energy-saving and emission reduction effects. Based on the results presented in this paper, the proposed technologies present substantial economic benefits for both new calciners and for retrofit projects.

7. References

1. Chi Mei, Ping Zhou, *Nonferrous Metallurgical Furnace Design Manual*, Changsha: Central South University Press, 2018:509 (in Chinese).
2. Pungkuntran Jaganathan, Carbon Footprint Reduction in Alumina Calciners. *TRAVAUX 52, Proceedings of the 41st International ICSOBA Conference*, Dubai, 5 - 9 November 2023.
3. Benny E. Raahauge and Devarajan Niranjan, Experience with Particle Breakdown in Gas Suspension Calciners, *TRAVAUX 44, Proceedings of 33rd International ICSOBA Conference*, Dubai, United Arab Emirates, 29 November – 1 December 2015.
4. Susanne Wind and Benny E. Raahauge, Energy Efficiency in Gas Suspension Calciners (GSC), *TMS Light Metals 2009*, edited by Geoff Bearne, pp.235-240.
5. Levin, I. and D. Brandon, Metastable alumina polymorphs: crystal structures and transition sequences. *Journal of the American Ceramic Society*, 1998. 81(8): p. 1995–2012
6. Bijun Wu, Formation mechanism of nitrogen oxides during combustion, *Electric Power Environmental Protection*, 2003(4): 9–12 (in Chinese).
7. D.Kunii and O.Levenspiel, Fluidization Engineering,Second Edition, Butterworth Heinemann Series in Chemical Engineering,1991.